

HOR1, VERT/HOR2 and HOR1/HOR2. All of the VERT/HOR1 correlation coefficients are  $< 0.7$  while for VERT/HOR2 and HOR1/HOR2 the figures are 98 and 96%, respectively. The rotation of the transmitted polarisation by scatterers along the transmission paths ensures that the signals are uncorrelated. Therefore this arrangement can be utilised as a diversity system since it provides highly uncorrelated signals.

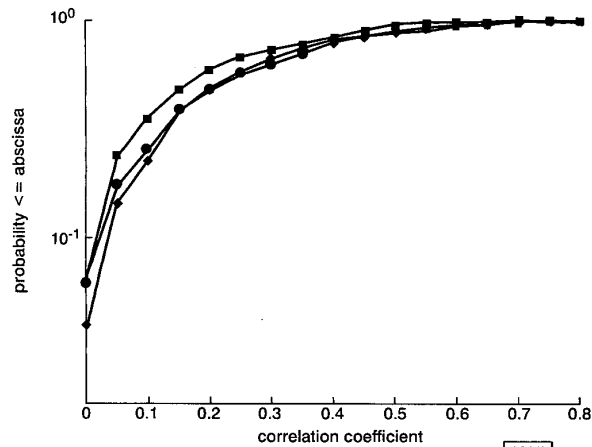


Fig. 2 Cumulative distributions of correlation coefficients

—■— VERT/HOR1  
—◆— VERT/HOR2  
—●— HOR1/HOR2

088/2

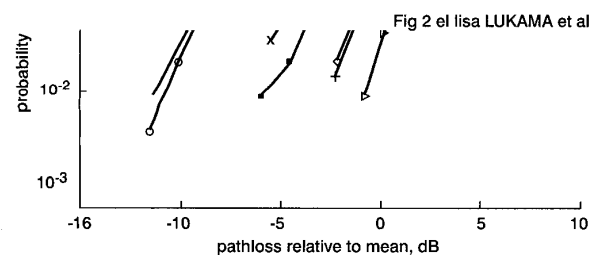


Fig. 3 Cumulative distributions of path losses with and without diversity

—■— VERT  
—○— HOR1  
—△— HOR2  
—◇— all channels  
—+— VERT and HOR1  
—+— VERT and HOR2  
—×— HOR1 and HOR2

The next step is to assess the gain that the system provides. This is done by analysing the power received by each antenna and employing some form of combining system. In this Letter, an equal gain combiner is assumed at the receiver. Measuring the diversity gains of the possible dual channel arrangements, i.e. VERT/HOR1, VERT/HOR2 and HOR1/HOR2 and comparing these to the three-branch scheme quantifies the improvement due to the extra branch. Fig. 3 shows the path losses of the different scenarios with and without diversity. It can be seen that at the 0.01 probability level or 99% signal reliability level, the vertically polarised receiver outperforms the horizontal receivers by  $\sim 5$  dB. A scheme employing the two horizontal antennas (HOR1/HOR2) is  $\sim 1$  dB poorer compared to the vertical antenna. However, by using the vertical antenna with either of the horizontal antennas (VERT/HOR1 or VERT/HOR2) a 3 dB improvement over the single vertical antenna is made. Employing all three antennas results in a 5 dB improvement over the single vertical antenna and 2 dB over the dual system. It is worth mentioning that the vertical

receiver dominates the horizontal antennas since the transmitted polarisation remains predominantly vertical. Therefore these results represent the worst-case scenario. In positions where the power on all the branches is almost equal, the diversity gain will be larger than above. Also, as the handset undergoes random orientation during use, the received power on the branches is likely to be equal over time. There are clear benefits of using a second horizontal antenna because the two antennas have been shown to be uncorrelated and receive almost the same power.

**Conclusions:** The performance of a three-branch orthogonal polarisation diversity system has been investigated and compared to that of a dual channel polarisation diversity system. The results show that the former system has a 2 dB advantage over the latter. Further, the received signals are highly uncorrelated. The above analysis is future-proof because broadband data has been used and could be applied to systems like 3G by downgrading the bandwidth to the specified value.

**Acknowledgments:** This work has been carried out as part of the British Telecommunications Virtual University Research Initiative on Mobility (BT VURI) and their continued support is highly appreciated. The authors would also like to acknowledge the financial support of the Rhodes Trust.

© IEE 2001

Electronics Letters Online No: 20010824  
DOI: 10.1049/el:20010824

26 February 2001

L. Lukama, K. Konstantinou and D.J. Edwards (Department of Engineering Science, University of Oxford, Parks Road, Oxford, OX1 3PJ, United Kingdom)

## References

- 1 LEE, W.C.: 'Mobile communications engineering' (McGraw-Hill Book Company, 1982)
- 2 LUKAMA, L., KONSTANTINO, K., and EDWARDS, D.J.: 'Polarization diversity performance for UMTS'. Int. Conf. Antennas and Propagation (ICAP2001), Manchester, UK, April 2001
- 3 VAUGHAN, R.G.: 'Polarization diversity in mobile communications', *IEEE Trans. Veh. Technol.*, 1990, 39, (3) pp. 177–186

## High-speed AlGaAs/GaAs HBTs with reduced base-collector capacitance

Woonyun Kim, Kyungho Lee, Minchul Chung, Jongchan Kang and Bumman Kim

A new layout for high-speed AlGaAs/GaAs heterojunction bipolar transistors (HBTs) is presented. The layout is horseshoe shaped and designed to simultaneously reduce base resistance ( $R_B$ ) and base-collector capacitance ( $C_{BC}$ ). A horseshoe-shaped HBT and a conventional single-finger HBT with the same emitter width of  $2 \mu\text{m}$  were fabricated and tested. The reduction of  $R_B$  and  $C_{BC}$  using the horseshoe-shaped HBT resulted in a 25% improvement of the maximum oscillation frequency ( $f_{max} = 130 \text{ GHz}$ ).

**Introduction:** Since heterojunction bipolar transistors (HBTs) were first suggested by Kroemer [1], much effort has been expended to develop high-speed HBTs. The process techniques to reduce base resistance ( $R_B$ ) and base-collector capacitance ( $C_{BC}$ ) such as isolation implantation of the extrinsic base and collector region [2, 3], laterally etched undercut [4, 5], epi regrowth for the thick base layer [6, 7], L-shaped base electrode [8], transferred-substrate technique [9], have contributed to remarkable improvement on device performance. However, an extensive study of the device layout to obtain a high-speed performance has yet to be made.

In this Letter, a new device layout structure for a high-speed HBT is presented. The layout seeks a reduced base-collector junction area, while simultaneously shortening the effective base length for a curtailment of the base metal resistance,  $R_{Bm}$ . The layout resembles a horseshoe. A horseshoe-shaped HBT and a conventional single-finger HBT with the same emitter size were fabricated and compared for high-speed performance. An  $f_{max}$  of 130 and

100 GHz for the horseshoe type and the single-finger HBTs, respectively, was achieved for  $2 \times 22 \mu\text{m}^2$  AlGaAs/GaAs HBTs, indicating that this layout is very favourable for high-speed HBTs. To our knowledge, these are one of the world-best results of the same size emitter HBTs fabricated without using special techniques such as the isolation implant process for extrinsic base-collector junction area.

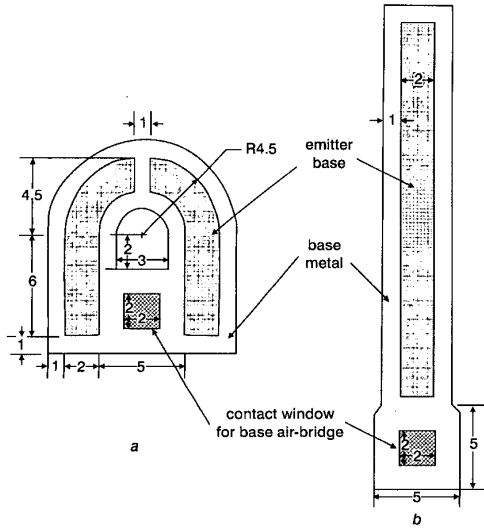


**Fig. 1** Basic features of HBTs with  $2 \times 22 \mu\text{m}^2$  emitter areas

a Horseshoe HBT  
b Single-finger HBT

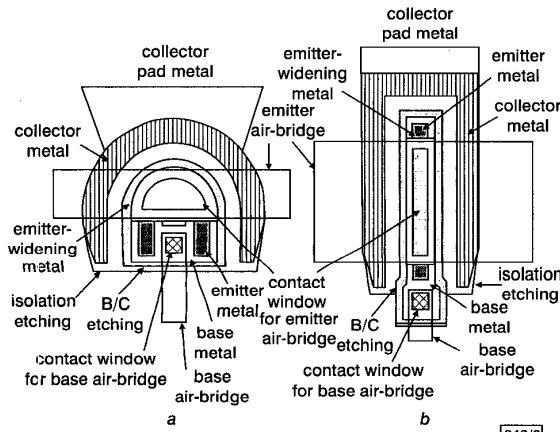


**Fig. 2** Layout of horseshoe and single-finger type HBTs with  $2 \times 22 \mu\text{m}^2$  emitter areas

a Horseshoe HBT  
b Single-finger HBT

**Table 1:** Epitaxial layer structures of AlGaAs/GaAs HBTs

Composition	Thickness $\mu\text{m}$	Concentration $\text{cm}^{-3}$	Dopant	Carrier type
$\text{Ga}_{1-y}\text{In}_y\text{As}$ ( $y = 0.5$ )	0.02	$2 \times 10^{19}$	Si	N
$\text{Ga}_{1-y}\text{In}_y\text{As}$ ( $y = 0.0 \rightarrow 0.5$ )	0.02	$2 \times 10^{19}$	Si	N
GaAs	0.09	$5 \times 10^{18}$	Si	N
GaAs	0.07	$5 \times 10^{17}$	Si	N
$\text{Ga}_{1-x}\text{Al}_x\text{As}$ ( $x = 0.3 \rightarrow 0.0$ )	0.03	$5 \times 10^{17}$	Si	N
$\text{Ga}_{1-x}\text{Al}_x\text{As}$ ( $x = 0.3$ )	0.07	$5 \times 10^{17}$	Si	N
GaAs	0.07	$5 \times 10^{19}$	C	P
GaAs	1.00/0.40	$2 \times 10^{16}$	Si	N
GaAs	0.60	$5 \times 10^{18}$	Si	N
S.I. substrate				

**Device design and fabrication:** The epitaxial layer structures are outlined in Table 1. Fig. 1 shows the basic features of the horseshoe type and single-finger type of HBT. Each HBT has  $44 \mu\text{m}^2$  emitter areas, but the layouts are quite different. The horseshoe type HBT has  $161 \mu\text{m}^2$  base-collector areas, while the single-finger type of HBT is  $190 \mu\text{m}^2$ . The longest path length of the base current in the horseshoe type HBT is about  $14 \mu\text{m}$ , while the single-finger device shows  $23 \mu\text{m}$ . Fig. 2 shows the layouts of the two HBTs. The emitter widening metal is used for an easy alignment of the following pattern. Emitter and base metals are connected to pad metals by Au air-bridges. Self-aligned HBTs were fabricated using contact alignment, with standard lift-off techniques for metallisations [10].

**Device performance:** The maximum current DC gains of the HBTs are approximately 30. The breakdown voltages of both types of HBTs at an open base,  $BV_{ce0}$ , are 10 V for the thin-collector HBT and 17 V for the thick-collector one. RF performances of the  $2 \times 22 \mu\text{m}^2$  emitter HBTs were measured using a network analyser from 0.1 to 40 GHz. Figs. 3a and b show a comparison of gain-frequency characteristics of the horseshoe type with the single-finger type. For HBTs with a collector thickness of  $1 \mu\text{m}$  the  $f_T$  and  $f_{max}$  are 52 and 105 GHz, respectively, at  $I_C = 16 \text{ mA}$  and  $V_{CE} = 2.3 \text{ V}$  for the single-finger type, and 50 and 130 GHz at the same bias point for the horseshoe type. For the  $0.4 \mu\text{m}$  thick-collector HBT the  $f_T$  and  $f_{max}$  are 67 and 60 GHz, respectively, at  $I_C = 18 \text{ mA}$  and  $V_{CE} = 2.0 \text{ V}$  for the single-finger type HBT, and 68 and 80 GHz at the same bias point for the horseshoe type. The  $f_{max}$ s are increased by about 25% as a result of the new layout.

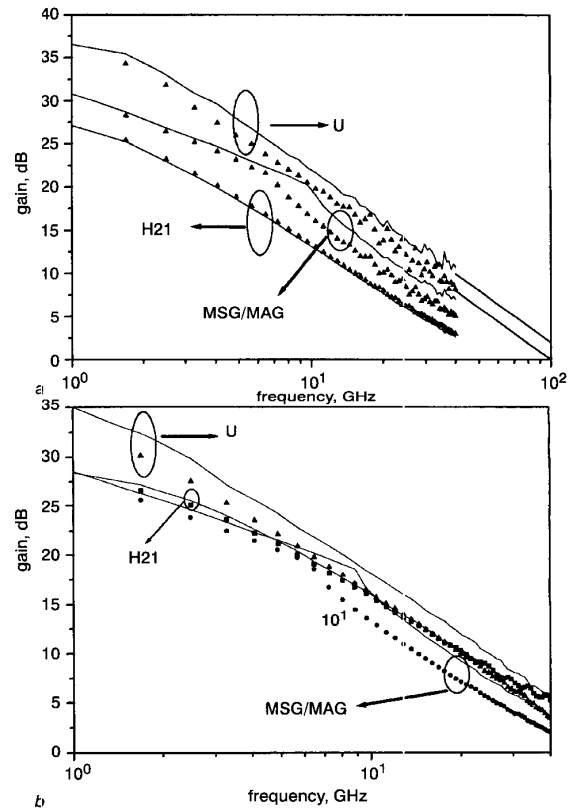


**Fig. 3** Microwave performance of horseshoe and single-finger type HBTs with  $2 \times 22 \mu\text{m}^2$  emitter areas

a HBTs with  $1.0 \mu\text{m}$  thick collector  
— horseshoe HBT  
▲ single-finger HBT  
b HBTs with  $0.4 \mu\text{m}$  thick collector  
— horseshoe HBT  
●▲ single-finger HBT

**Conclusion:** A new device layout for high-speed AlGaAs/GaAs HBTs using a simple process technique has been presented. This layout is horseshoe shaped and designed to simultaneously reduce base resistance ( $R_B$ ) and base-collector capacitance ( $C_{BC}$ ). A horse-

shoe-shaped HBT and a conventional single-finger HBT with the same emitter width of 2  $\mu\text{m}$  were fabricated for comparison. The  $f_T$  and  $f_{max}$  are 52 and 105 GHz, respectively at  $I_C = 16\text{ mA}$  and  $V_{CE} = 2.3\text{ V}$  for the single-finger type of HBT with 1  $\mu\text{m}$  thick collector, and 50 and 130 GHz at the same bias point for the comparable horseshoe type HBT.

**Acknowledgments:** This work was supported in part by the Agency for Defense Development and the Brain Korea 21 Project of the Ministry of Education. The authors would like to thank H.C. Seo, Eoncom Ltd., for his assistance with the sawing process.

© IEE 2001

Electronics Letters Online No: 20010835  
DOI: 10.1049/el:20010835

12 February 2001

Woonyun Kim, Kyungho Lee, Minchul Chung, Jongchan Kang and Bumman Kim (Department of Electronics and Electrical Engineering and Microwave Application Research Center, Pohang University of Science and Technology, San 31, Hyoja-dong, Nam-gu, Pohang, Kyungbuk, 790-784, Republic of Korea)

## References

- 1 KROEMER, H.: 'Heterojunction bipolar transistors and integrated circuits', *Proc. IEEE*, 1982, **70**, (1), pp. 13–25
- 2 NAKAJIMA, O., NAGATA, K., YAMAGUCHI, Y., ITO, H., and ISHIBASHI, T.: 'Improvement in AlGaAs/GaAs HBT power gains with buried proton-implanted layer', *Electron. Lett.*, 1986, **22**, (25), pp. 1317–1318
- 3 HO, M.C., JOHNSON, R.A., CHANG, C.E., HO, W.J., PEHLKE, D.R., ZAMPARDI, P.J., CHANG, M.F., and ASBECK, P.M.: 'Base-collector capacitance reduction of AlGaAs/GaAs heterojunction bipolar transistors by deep ion implantation'. *Device Res. Conf. Dig.*, 1995, pp. 86–87
- 4 CHEN, W.L., CHAU, H.F., TUTT, M., HO, M.C., KIM, T.S., and HENDERSON, T.: 'High-speed InGaP/GaAs HBTs using a simple collector undercut technique to reduce base-collector capacitance', *IEEE Electron. Device Lett.*, 1997, **18**, (7), pp. 355–357
- 5 LIU, W., HILL, D., CHAU, H.-F., SWEDER, J., NAGLE, T., and DELANEY, J.: 'Laterally etched undercut (LEU) technique to reduce base-collector capacitances in heterojunction bipolar transistors'. *IEEE GaAs IC Symp. Dig.*, 1995, pp. 167–170
- 6 ENQUIST, P.M., SLATER, D.B., JR., HUTCHBY, J.A., MORRIS, A.S., and TREW, R.J.: 'Self-aligned AlGaAs/GaAs HBT with selectively regrown OMVPE emitter', *IEEE Electron. Device Lett.*, 1993, **14**, (6), pp. 295–297
- 7 SHIMAWAKI, H., AMAMIYA, Y., FURUHATA, N., and HONJO, K.: 'High-fmax AlGaAs/InGaAs and AlGaAs/GaAs HBTs with p+/p regrown base contacts', *IEEE Trans. Electron Devices*, 1995, **42**, (10), pp. 1735–1744
- 8 YANAGIHARA, M., SAKAI, H., OTA, Y., TANABE, M., INOUE, K., and TAMURA, A.: '253-GHz fmax AlGaAs/GaAs HBT with Ni/Ti/Pt/Ti/Pt-contact and L-shaped base electrode'. *Tech. Dig. IEEE IEDM*, 1990, pp. 807–810
- 9 RODWELL, M., BETSER, Y., JAGANATHAN, S., MATHEW, T., SUNDARARAJAN, P.K., MARTIN, S.C., SMITH, R.P., WEI, Y., URTEAGA, M., SCOTT, D., and LONG, S.: 'Submicron lateral scaling of HBTs and other vertical-transport devices: towards THz bandwidths'. *GaAs 2000 Conf. Proc.*, Paris, France, Oct. 2000, pp. 1–2
- 10 LEE, J., KIM, W., KIM, Y., RHO, T., and KIM, B.: 'Intermodulation mechanism and linearization of AlGaAs/GaAs HBTs', *IEEE Trans. Microw. Theory Tech.*, 1997, **45**, (12), pp. 2065–2072

## Inductively-loaded half-bridge inverter characterisation of 4H-SiC merged PiN/Schottky diodes up to 230 A and 250°C

P. Alexandrov, J.H. Zhao, W. Wright, M. Pan and M. Weiner

4H-SiC merged PiN/Schottky diodes were characterised in an inductively-loaded half-bridge inverter circuit at high current and high temperatures (high-T) for the first time. Results show that the replacement of Si freewheeling diodes by SiC diodes results in far less storage charges in the freewheeling diodes and substantial reduction in diode turn-off energy loss, especially at high-T.

**Introduction:** The SiC merged PiN/Schottky diode (MPSD) is an attractive device since it combines the best features of the PiN diode (PND) and the Schottky barrier diode (SBD) [1]. Fig. 1 shows the cross-sectional view of an MPSD, in which the top surface region consisting of the SBD is interspersed with islands of implanted p+ regions. In addition to its low forward voltage drop  $V_F$  and low reverse leakage current  $I_R$ , the MPSD also shares another desirable feature with the unipolar SBD, namely, extremely fast recovery. Since the MPSD forward current  $I_F$  is dominated by the SBD properties, there is very little carrier storage and indeed extremely fast recovery has been noted [2]. MPSD recovery measurements, however, have been limited to either low  $I_F$  or low current densities  $J_F$  of around 100 A/cm<sup>2</sup>. In system applications where current overshoot could lead to higher  $J_F$  (with higher  $V_F$ ), the current contribution due to the pn junction in an MPSD may degrade and slow down the recovery. In this Letter, we address this issue, and we investigate the recovery of MPSD at different temperatures with a  $J_F$  up to 2447 A/cm<sup>2</sup>.

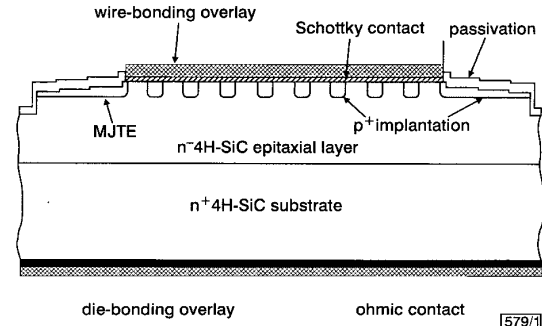


Fig. 1 Schematic cross-sectional view of 4H-SiC MPS diode

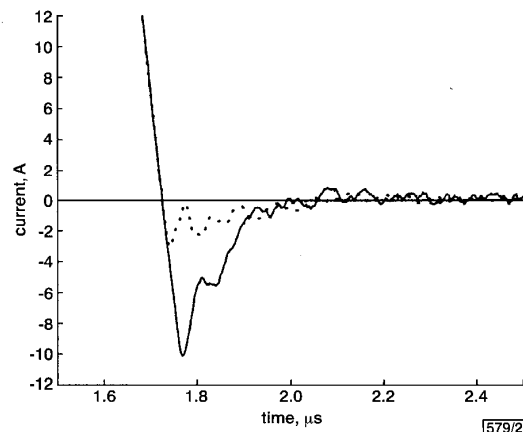


Fig. 2 Expanded detailed reverse recovery current of 4H-SiC MPS diode and ultrafast soft recovery Si PiN diode measured at RT

Switching voltage 400 V, switching current 250 A

— Si PiN ( $Q_{rr} = 0.97\ \mu\text{C}$ )  
--- SiC MPS ( $Q_{rr} = 0.30\ \mu\text{C}$ )

**MPS diode design parameters:** The p+ implanted regions and the multistep junction termination extension (MJTE) sections were designed in the form of concentric rings. MJTE was introduced to increase blocking voltage and reduce reverse leakage. The width of the p+ concentric rings was 1.5  $\mu\text{m}$ . The Schottky ring width was 3  $\mu\text{m}$ . The thickness and doping for the drift layer were 6  $\mu\text{m}$  and  $n = 2.1 \times 10^{16}\text{ cm}^{-3}$ , respectively. The Al implantation had a concentration of  $2 \times 10^{18}\text{ cm}^{-3}$  and a depth of 1.3  $\mu\text{m}$ . The cell diameter was 1 mm. Multicell packaged devices were fabricated, each consisting of twelve 1 mm cells, with a total active area of 9.4 mm<sup>2</sup>.

**Experimental results:** The packaged devices were evaluated in an inductively-loaded ( $L = 1000\ \mu\text{H}$ ) half-bridge circuit [3], consisting of a pair of Si IGBT switches and free-wheeling diodes. The diode turn-off was tested from room temperature (RT) up to 250°C. The switching voltage was 400 V. The maximum tested on-state current was 230 A at RT, corresponding to a  $J_F = 2447\text{ A/cm}^2$  and 150 A